

# A Semiparametric Bayesian Model for Neural Coding

Babak Shahbaba\*, Bo Zhou\*, Hernando Ombao\*, David Moorman†,  
and Sam Behseta‡

September 20, 2022

## Abstract

We propose a semiparametric Bayesian model to capture dependencies among multiple neurons by detecting their co-firing (possibly with some lag time) patterns over time. After discretizing time so there is at most one spike at each interval, the resulting sequence of 1's (spike) and 0's (silence) for each neuron is modeled using the logistic function of a continuous latent variable with a Gaussian process prior. For multiple neurons, the corresponding marginal distributions is coupled to their joint probability distribution using a parametric copula model. This way, while the nonparametric component (i.e., the Gaussian process model) provides a flexible framework for modeling the underlying firing rates, the parametric component (i.e., the copula model) allows us to make inference regarding the relationships among neurons. Using simulated data, we show that our approach could correctly capture temporal dependencies in firing rates and identify synchronous neurons. We also apply our model to data obtained from prefrontal cortical areas.

## 1 Introduction

Neurophysiological studies commonly involve modeling a sequence of spikes (action potentials) over time, known as a *spike train*, for each neuron. Complex behaviors, however, are driven by networks of neurons. To this end, we propose a flexible, yet robust semiparametric Bayesian method for capturing temporal cross-dependencies among multiple neurons by simultaneous modeling of their spike trains.

Capturing the dynamics of neuronal networks partly depends on a better understanding of the temporal correlations between their associated spike trains. A way of decoding such associations is to distinguish *exact synchrony* or *lagged synchrony* between a pair of neurons, from the correlated firing. According to [1], synchronous firing patterns were initially investigated with exploratory graphical tools, such as the cross-correlation histogram, and Joint Peristimulus Time Histogram (JPSTH) [2]. Subsequently, a class of associated ad-hoc methods were developed for addressing the question of whether exact or lagged synchrony in a pair of neurons is merely due

---

\*Department of Statistics, UC Irvine, CA, USA

†Department of Neurosciences, Medical University of South Carolina, Charleston, SC, USA

‡Department of Mathematics, California State University, Fullerton, CA, USA

to chance. To explore the related hypothesis, a host of resampling methods such as bootstrap confidence intervals were introduced [1]. Later on, trial to trial variability models were utilized to model the evolving intensity of firing rates between multiple trials. For more discussion on analysis of spike trains, refer to [1, 3, 4, 5, 6, 7, 8, 9, 10, 11].

Recently, Kelly and Kass [12] proposed a new method to quantify synchrony. They argue that separating stimulus effects from history effects would allow for a more precise estimation of the instantaneous conditional firing rate. Specifically, given the firing history  $H_t$ , suppose  $\lambda^A(t|H_t^A)$ ,  $\lambda^B(t|H_t^B)$ , and  $\lambda^{AB}(t|H_t^{AB})$  are the conditional firing intensities of neuron A, neuron B, and their synchronous spikes respectively. Independence between the two point processes can be examined by testing the null hypothesis  $H_0 : \zeta(t) = 1$ , where  $\zeta(t) = \frac{\lambda^{AB}(t|H_t^{AB})}{\lambda^A(t|H_t^A)\lambda^B(t|H_t^B)}$ . The quantity  $[\zeta(t) - 1]$  can be interpreted as the excess proportion of co-firing above what is predicted by independence. Note that we still need to model the marginal probability of firing for each neuron. To do this, one could assume that a spike train follows a Poisson process, which is the simplest form of point processes. By doing so, we are in fact assuming that the number of spikes within a particular time frame follows a Poisson distribution. It is, however, very unlikely that actual spike trains follow this assumption [13, 14, 15, 5, 16]. One possible remedy is to use inhomogeneous Poisson process, which assumes time-varying firing rates. See [3, 4, 5, 6, 7, 17, 18, 19, 20, 11] for more alternative methods for modeling spike trains.

In this paper, we propose a new semiparametric method for neural decoding. To this end, we first discretize time so that there is at most one spike within each time interval and let the response variable to be a binary process comprised of 1s and 0s. We then use a continuous latent variable with Gaussian process prior to model the time-varying and history-dependent firing rate for each neuron. The covariance function for the Gaussian process is specified in a way that it creates prior positive autocorrelation for the latent variable so the firing rate could depend on spiking history. For each neuron, the marginal probability of firing within an interval is equal to the logistic function of its corresponding latent variable. A parametric copula model connects the joint distribution of spikes for multiple neurons to their marginals in order to capture their cross-dependencies. Additionally, our model allows for co-firing of neurons after some lag time.

Throughout this paper, we evaluate our proposed method using simulated data and apply it to real data based on an experiment investigating the role of prefrontal cortical area in rats with respect to reward-seeking behavior and inhibition of reward-seeking in the absence of a rewarded outcome. In this experiment, the activity of 5-25 neurons from prefrontal cortical area was recorded. During recording, rats chose to either press or withhold presses to presented levers. Pressing lever 1 allowed the rat to acquire a sucrose reward while pressing lever 2 had no effect. (All protocols and procedures followed National Institute of Health guidelines for the care and use of laboratory animals.)

In what follows, we first describe our Gaussian process model for the firing rate of a single neuron (Section 2). In Section 3, we present our method for detecting co-firing (possibly after some lag time) patterns for two neurons, and evaluate its performance in Section 4. The extension of this method for multiple neurons is presented in Section 5. Finally, in Section 6, we discuss future directions.

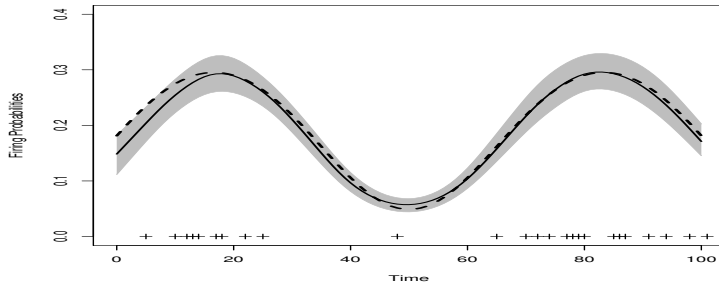


Figure 1: An illustrative example for using a Gaussian process model for a neuron with 40 trials. The dashed line shows the true firing rate, the solid line shows the posterior expectation of the firing rate, and the gray area shows the corresponding 95% probability interval. The plus signs on the horizontal axis represents spikes over 100 time intervals for one of the 40 trials.

## 2 Gaussian process model of firing rates

We use a Gaussian process model for each neuron’s firing rate. To this end, we first discretize time so that there is at most one spike within each time interval and let the response variable,  $Y$ , to be a binary process comprised of 1s (spike) and 0s (silence). We assume that the firing rate for each neuron depends on an underlying latent variable,  $u(t)$ , with a Gaussian process prior. In Statistics and Machine Learning, Gaussian processes are widely used as priors over functions. Similar to the Gaussian distribution, a Gaussian process is defined by its mean (usually set to 0 in prior) and its covariance function  $C$ :  $u(t) \sim \mathcal{GP}(0, C)$ . For the problems discussed here, the stochastic process is indexed by time  $t$ ; hence, the covariance function is defined in terms of  $t$ . We use the following covariance form, which includes a wide range of smooth nonlinear functions [21, 22]:

$$\begin{aligned} C_{ij} &= \text{Cov}[u(t_i), u(t_j)] \\ &= \lambda^2 + \eta^2 \exp[-\rho^2(t_i - t_j)^2] + \delta_{ij}\sigma_\varepsilon^2 \end{aligned}$$

Here,  $\lambda, \eta, \rho$ , and  $\sigma$  are hyperparameters with their own hyperpriors. We use  $p_t$  to denote the spike probability within time interval  $t$  and define it as follows:

$$p_t = \frac{1}{1 + \exp[-u(t)]}$$

When there are  $R$  trials (i.e.,  $R$  spike trains) for each neuron, we model the corresponding spike trains as conditionally independent given the latent variable  $u(t)$ . Figure 1 illustrates this method using 40 simulated spike trains for a single neuron. Note that we can allow for trial-to-trial variation by including a trial-specific mean parameter such that  $[u(t)]^{(r)} \sim \mathcal{GP}(\mu_r, C)$ , where  $r = 1, \dots, R$ .

### 3 Modeling dependencies between two neurons

Let  $Y$  be the observed spike train of the first neuron, and  $Z$  be the observed spike train of the second neuron. Here,  $y_t$  and  $z_t$  are binary data indicating presence or absence of spikes within time interval  $t$ . We use  $p_t$  to denote the spike probability at interval  $t$  for the first neuron, and  $q_t$  to denote the spike probability at the same interval for the second neuron. Given the corresponding latent variables  $u(t)$  and  $v(t)$  with Gaussian process priors  $\mathcal{GP}(0, C_u)$  and  $\mathcal{GP}(0, C_v)$  respectively, we model these probabilities as  $p_t = 1/\{1 + \exp[-u(t)]\}$  and  $q_t = 1/\{1 + \exp[-v(t)]\}$ .

If the two neurons are independent, the probability of firing at the same time is  $P(y_t = 1, z_t = 1) = p_t q_t$ . In general, however, we can write the probability of firing at the simultaneously as the product of their individual probabilities multiplied by a factor,  $\zeta$ , which represents the excess firing rate due to dependence between two neurons [23, 12]. That is,  $\zeta$  accounts for the excess joint spiking beyond what explained by independence. For independent neurons,  $\zeta = 1$ . The extra firing can occur after some lag time  $L$ ; that is, in general  $P(y_t = 1, z_{t+L} = 1) = p_t q_{t+L} \zeta$  for some  $L$ . Therefore, the marginal and joint probabilities are

$$\begin{aligned}
 P(y_t = 1|p, q, \zeta, L) &= p_t \\
 P(y_t = 0|p, q, \zeta, L) &= 1 - p_t \\
 P(z_t = 1|p, q, \zeta, L) &= q_t \\
 P(z_t = 0|p, q, \zeta, L) &= 1 - q_t \\
 P(y_t = 1, z_{t+L} = 1|p, q, \zeta, L) &= p_t q_{t+L} \zeta \\
 P(y_t = 1, z_{t+L} = 0|p, q, \zeta, L) &= p_t - p_t q_{t+L} \zeta \\
 P(y_t = 0, z_{t+L} = 1|p, q, \zeta, L) &= q_t - p_t q_{t+L} \zeta \\
 P(y_t = 0, z_{t+L} = 0|p, q, \zeta, L) &= 1 - p_t - q_t + p_t q_{t+L} \zeta
 \end{aligned}$$

We assume that  $L$  can take a finite set of values from  $[-K, K]$  for some predefined  $K$  and write the likelihood function as follows:

$$\begin{aligned}
 &\sum_{k=0}^K 1_{k=L} \prod_{r=1}^R \left[ \prod_{t=1}^{T-L} P(y_t^{(r)}, z_{t+L}^{(r)}) \prod_{t=T-L+1}^T P(y_t^{(r)}) \prod_{t=1}^L P(z_t^{(r)}) \right] + \\
 &\sum_{k=-K}^{-1} 1_{k=L} \prod_{r=1}^R \left[ \prod_{t=1}^{T+L} P(y_{t-L}^{(r)}, z_t^{(r)}) \prod_{t=1}^{-L} P(y_t^{(r)}) \prod_{t=T+L+1}^T P(z_t^{(r)}) \right]
 \end{aligned}$$

We put a discrete uniform prior distribution on  $L$  and assume weakly informative priors for  $\zeta$  and the hyperparameters in covariance functions. We use Markov Chain Monte Carlo algorithms to simulate samples from the posterior distribution of model parameters given the observed spike trains.

#### 3.1 Illustrative examples

In this section, we use simulated data to illustrate our method. We consider three scenarios: 1) two independent neurons, 2) two dependent neurons with exact synchrony ( $L = 0$ ), and 3) Two dependent neurons with lagged co-firing. In each scenario, we assume a time-varying firing rate for each neuron and simulate 40 spike trains given the underlying firing rate. For independent neurons, we set  $\zeta = 1$ , whereas  $\zeta > 1$  for dependent neurons.

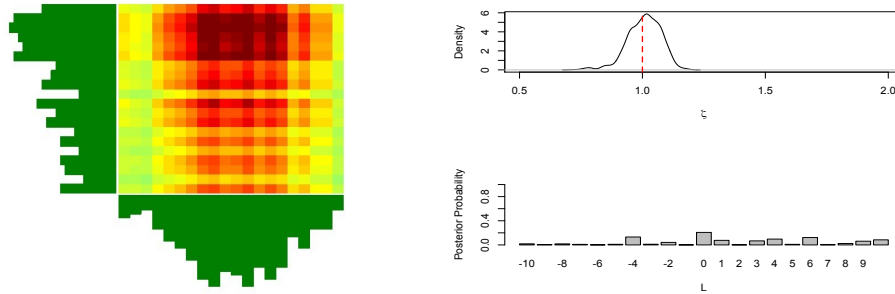


Figure 2: **Two independent neurons**– The left panel shows the corresponding JPSTH. The right panel shows the posterior distributions of  $\zeta$  and  $L$ .

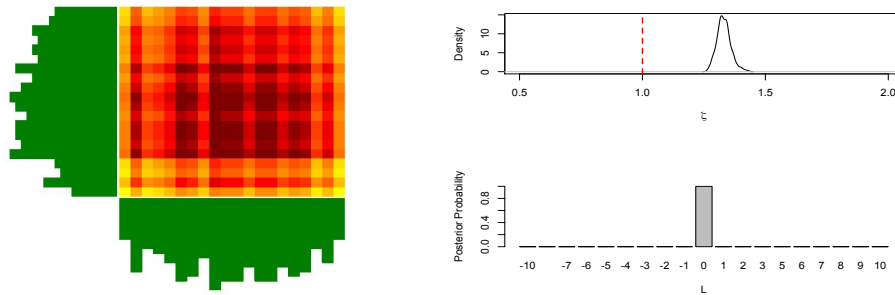


Figure 3: **Two dependent neurons in exact synchrony**– The left panel show the frequency of spikes over time. The right panel shows the posterior distribution of  $\zeta$  and  $L$ .

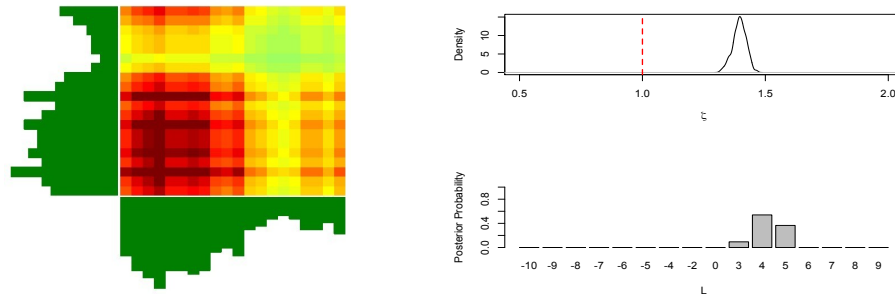


Figure 4: **Two dependent neurons in lagged synchrony**– For different trials, the lag values are randomly set to 3, 4, or 5 with probabilities 0.2, 0.5, and 0.3 respectively. The left panel show the frequency of spikes over time. The right panel shows the posterior distribution of  $\zeta$  and  $L$ .

**Two independent neurons** In the first scenario, we consider two independent neurons. The left panel of Figure 2 shows the corresponding Joint Peristimulus Time Histogram (JPSTH). Each cell represents the joint frequency of spikes (darker cells represent higher frequencies) for the two neurons at given times. The marginal distributions of spikes, i.e., Peristimulus Time Histogram (PSTH), for the first neuron is shown along the horizontal axis. The second neuron’s PSTH is shown along the vertical axis. The right panel of Figure 2 shows the posterior distributions of  $\zeta$  and  $L$ . For this example, the posterior distribution of  $\zeta$  is concentrated around 1 with median and 95% posterior probability interval equal to 1.01 and [0.85,1.12] respectively. This overwhelmingly suggests that the two neurons are independent as expected. Further, the posterior probabilities of all lag values from -10 to 10 are quite small.

**Two synchronous neurons** For our next example, we simulate data for two dependent neurons with synchrony (i.e.,  $L = 0$ ). We set  $\zeta = 1.6$ . That is, the probability of co-firing at the same time is 60% higher than that of independent neurons. Figure 3 shows their corresponding JPSTH along with the posterior distributions of  $\zeta$  and  $L$ . In this case, the posterior median and 95% posterior probability interval for  $\zeta$  are 1.33 and [1.28,1.40]. Therefore,  $\zeta$  identifies the two neurons as dependent. Further, the posterior distribution of  $L$  shows that the two neurons are in exact synchrony.

**Two dependent neurons with lagged co-firing** Similar to the previous example, we set the probability of co-firing 60% higher than what we obtain by the independence assumption. However, In this case, the second neuron tends to fire after some lag time,  $L$ . For different trials, we randomly set  $L$  to 3, 4, or 5 with probabilities 0.2, 0.5, and 0.3 respectively. Figure 4 shows JPSTH along with the posterior distributions of  $\zeta$  and  $L$ . As before, the posterior distribution of  $\zeta$  can be used to detect the relationship between the two neurons. For this example, the posterior median and 95% posterior interval for  $\zeta$  are 1.39 and [1.33,1.44] respectively. Also, our method could identify the three lag values correctly.

## 4 Experimental results

In this section, we evaluate the performance of our proposed approach by comparing it to the method of Kass et. al. [24] in terms of statistical power for detecting synchronous neurons. We also apply our method to the real data we discussed in the introduction.

### 4.1 Power analysis

We use two simulation studies to compare our approach to that of Kass et. al. [24]. In their approach, Kass et. al. [24] find the marginal firing rate of each neuron using natural cubic splines and then evaluate the amount of excess joint spiking using the bootstrap method. Therefore, for our first simulation study, we generate datasets that conform with the underlying assumptions of both methods. More specifically, we first generate the marginal firing rates for both neurons, and then generate the spike trains for two neurons given  $\zeta$  (i.e., excess joint firing rate). The left panel of Figure 5 compares the two methods in terms of statistical power for different values of

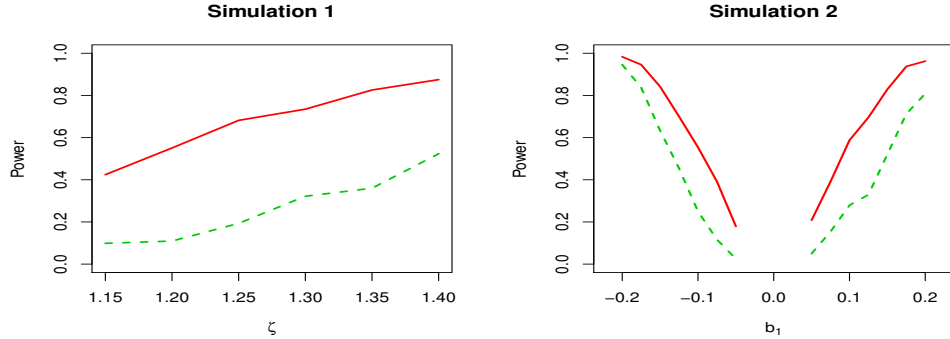


Figure 5: **Power analysis**– Comparing our proposed method (solid curves) to the method of [24] (dashed curves) based on statistical power using two simulation studies.

$\zeta$  using 200 simulated datasets each with 20 trials. As we can see, our method (solid curve) has substantially higher power compared to the method of [24] (dashed curve).

For our second simulation, we generate datasets that do not conform with the underlying assumptions of the two methods. Let  $Y = (y_1, \dots, y_T)$  and  $Z = (z_1, \dots, z_T)$  denote the spike trains for two neurons. We first simulate  $y_t$ , i.e., absence or presence of spikes for the first neuron at time  $t$ , from  $\text{Bernoulli}(p_t)$ , where  $p_t = 0.25 - 0.1 \cos(12\pi t)$  for  $t \in [0, 0.2]$ . Then, we simulate  $z_t$  for the second neuron from  $\text{Bernoulli}(b_0 + b_1 y_t)$  for given values of  $b_0$  and  $b_1$ . We set  $b_0$  (i.e., the baseline probability of firing for the second neuron) to 0.2. When  $b_1 = 0$ , the two neurons are independent. Positive values of  $b_1$  leads to higher rates of co-firing between the two neurons. When  $b_1$  is negative, the first neuron has an inhibitory effect on the second neuron. The right panel of Figure 5 compares the two methods in terms of statistical power for different values of  $b_1$  using 200 simulated datasets each with 20 trials. As before, our method (solid curves) has higher statistical power compared to the method of [24] (dashed curves).

## 4.2 Results for real data

We now use our method for analyzing a pair of neurons selected from the experiment discussed in the introduction. (We will apply our method to multiple neurons in the next section.) Although we applied our method to several pairs with different patterns, for brevity we present the results for one pair of neurons whose relationship changes under different scenarios. For non-rewarded stimulus (lever 2), the posterior median and 95% probability intervals for  $\zeta$  are 1.84 and [1.69, 2.00] respectively. This is further confirmed by the plots of the number of co-firings and correlation coefficients for different lags presented in Figure 6. The right panel of this figure shows the estimated conditional probabilities (using the sample proportions) of firing for the second neuron given the firing status of the first neuron for different lags; the solid line shows these estimated probabilities when the first neuron is silent whereas the dashed line shows the estimated probabilities when the first neuron spikes. Around lag zero, the estimated probabilities are substantially different.

Figure 7 shows the corresponding plots for these two neurons under the rewarded-stimulus scenario. This time, the two neurons do not seem to be related. This is confirmed by our model:

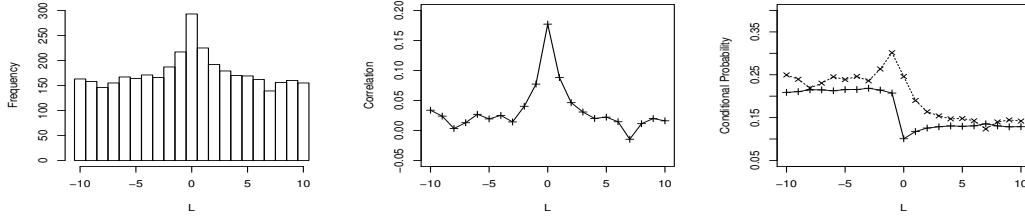


Figure 6: **Non-rewarded Stimulus**– The co-firing frequencies (Left), correlation coefficients (Middle), and estimated conditional probabilities of firing for the second neuron given the firing status (0: solid line, 1: dashed line) of the first neuron (Right) over different lag values ( $L$ ).

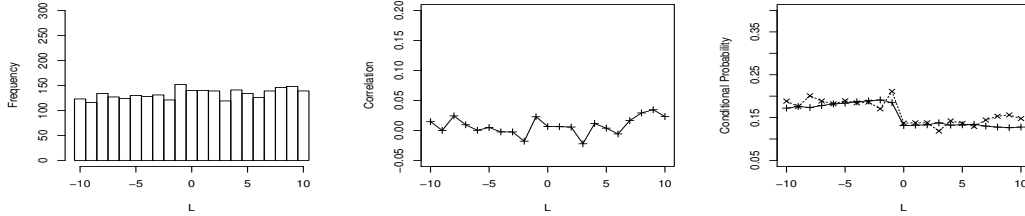


Figure 7: **Rewarded Stimulus**– The co-firing frequencies (Left), correlation coefficients (Middle), and estimated conditional probabilities of firing for the second neuron given the firing status (0: solid line, 1: dashed line) of the first neuron (Right) over different lag values ( $L$ ).

the posterior median and 95% probability interval for  $\zeta$  are 1.12 and  $[0.88, 1.31]$  respectively.

## 5 Modeling dependencies among multiple neurons

Temporal relationships among neurons, particularly those that change across different contexts, can provide additional information beyond basic firing rate. Because it is possible to record spike trains from multiple neurons simultaneously, and because network encoding likely spans more than pairs of neurons, we now turn our attention to calculating temporally-related activity among multiple ( $> 2$ ) simultaneously-recorded neurons.

At lag zero (i.e.,  $L = 0$ ), we can rewrite our model for the joint distribution of two neurons in terms of their individual cumulative distributions as follows (we have dropped the index  $t$  for simplicity):

$$H(y, z) = \mathcal{C}(F_1(y), F_2(z)) = \left[1 + \beta \prod_{i=1}^2 (1 - F_i)\right] \prod_{i=1}^2 F_i$$

where  $F_1 = F_1(y) = P(Y \leq y)$ ,  $F_2 = F_2(z) = P(Z \leq z)$ , and  $\beta = \frac{\xi-1}{(1-p)(1-q)}$ . Note that in this case,  $\beta = 0$  indicates that the two neurons are independent. In general, models that couple the joint distribution of two (or more) variables to their individual marginal distributions are called copula models. See [25] for detailed discussion of copula models. Let  $H$  be  $n$ -dimensional distribution functions with marginals  $F_1, \dots, F_n$ . Then, an  $n$ -dimensional copula is a function of the following



Table 1: Estimates of  $\beta$ 's along with their 95% probability intervals for simulated data based on our copula-based model. Here, row  $i$  column  $j$  shows  $\beta_{ij}$ , which captures the relationship between the  $i^{th}$  and  $j^{th}$  neurons.

$\beta$	2	3	4
1	<b>1.41(1.09,1.75)</b>	-0.02(-0.34,0.32)	0.00(-0.28,0.35)
2		-0.24(-0.57,0.08)	-0.24(-0.49,0.04)
3			<b>1.49(1.15,1.86)</b>

form:

$$H(y_1, \dots, y_n) = \mathcal{C}(F_1(y_1), \dots, F_n(y_n)), \text{ for all } y_1, \dots, y_n$$

Here,  $\mathcal{C}$  defines the dependence structure between the marginals. Our model for two neurons is in fact a special case of the Farlie-Gumbel-Morgenstern (FGM) copula family [26, 27, 28, 25]. For  $n$  random variables  $Y_1, Y_2, \dots, Y_n$ , the FGM copula,  $\mathcal{C}$ , has the following form:

$$\left[1 + \sum_{k=2}^n \sum_{1 \leq j_1 < \dots < j_k \leq n} \beta_{j_1 j_2 \dots j_k} \prod_{l=1}^k (1 - F_{j_l})\right] \prod_{i=1}^n F_i$$

where  $F_i = F_i(y_i)$ . Restricting our model to second-order interactions, we can generalize our approach for two neurons to a copula-based model for multiple neurons using the FGM copula family,

$$H(y_1, \dots, y_n) = \left[1 + \sum_{1 \leq j_1 < j_2 \leq n} \beta_{j_1 j_2} \prod_{l=1}^2 (1 - F_{j_l})\right] \prod_{i=1}^n F_i$$

where  $F_i = P(Y_i \leq y_i)$ . Here, we use  $y_1, \dots, y_n$  to denote the firing status of  $n$  neurons at time  $t$ ;  $\beta_{j_1 j_2}$  captures the relationship between the  $j_1^{th}$  and  $j_2^{th}$  neurons.

## 5.1 Illustrative example

To illustrate this method, we follow a similar procedure as Scenario 2 in Section 3.1 and simulate spike trains for four neurons such that neurons 1 is in exact synchrony with neuron 2, and neurons 3 is in exact synchrony with neuron 4. The two pairs are however independent from each other. Table 1 shows the estimated  $\beta$ 's along with their corresponding 95% probability intervals. Our method correctly detects the relationship among the neurons: for synchronous neurons, the corresponding  $\beta$ 's are significantly larger than 0 (i.e., 95% probability intervals do not include 0), whereas the remaining  $\beta$ 's are close to 0 (i.e., 95% probability intervals include 0).

## 5.2 Results for real data

We now use our copula-based method for analyzing our experimental data. As mentioned above, during task performance we recorded the activity of 5-25 neurons under two conditions: rewarded

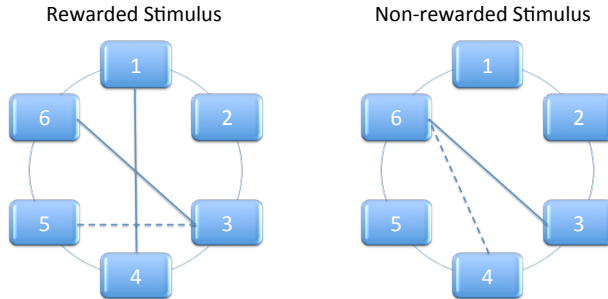


Figure 8: A schematic representation of connections between six neurons under two experimental conditions. The solid line indicate positive association ( $\beta$  is significantly above zero), whereas the dashed line indicate negative association ( $\beta$  is significantly less than zero).

stimulus (lever 1) and non-rewarded stimulus (lever 2). Here, we focus on 6 simultaneously recorded neurons. There are 54 trials for each condition. Figure 8 illustrates our findings. As we can see, there are differences in relationships among neurons depending on context. Although neurons 3 and 6 are positively correlated for presentation of both lever 1 and lever 2, the negative correlations (between 3 and 5 for lever 1 and between 4 and 6 for lever 2) serve as additional information that can be used to distinguish behavioral contexts. The results of these analyses are important since they argue that neurons perform multiple functions depending on the network in which they are participating. Therefore, characterizing the temporal relationships in activity across many neurons is more informative than looking at single neurons or even pairs.

## 6 Discussion

The analysis results presented here have demonstrated a number of ways in which examining the temporal relationship of activity in multiple neurons can reveal information about population dynamics of neuronal circuits. These kinds of data are critical in going beyond treating populations as averages of single neurons, as is commonly done in physiological studies.. As discussed above, these results unveil how neurons within a brain region interrelate. Although more investigations are needed in larger populations of neurons to develop our understanding of population dynamics, the tools displayed here allow us to interrogate the relationship of interconnected neurons as a coding variable.

In our current model,  $\zeta$  is constant. However, dependencies among neurons could in fact change over time. To address this issue, we could allow  $\beta$ 's to be piecewise constant over time to capture non-stationary neural connections. Change-point detection would of course remain a challenge.

Finally, our proposed models tend to be computationally intensive. This fact becomes even more salient given that current technology allow the simultaneous recording of many neurons. Faster exploration of parameter space can be obtained using more efficient sampling algorithms [29].

## References

- [1] M. T. Harrison, A. Amarasingham, and R. E. Kass. Statistical identification of synchronous spiking. In P. Di Lorenzo and J. Victor., editors, *Spike Timing: Mechanisms and Function*. Taylor and Francis, 2013.
- [2] G. L. Gerstein and D. H. Perkel. Simultaneously recorded trains of action potentials: Analysis and functional interpretation. *Science*, 164(3881):828–830, 1969.
- [3] D. R. Brillinger. Maximum likelihood analysis of spike trains of interacting nerve cells. *Biological Cybernetics*, 59:189–200, 1988.
- [4] E. N. Brown, R. E. Kass, and P. P. Mitra. Multiple neural spike train data analysis: state-of-the-art and future challenges. *Nature Neuroscience*, 7(5):456–461, 2004.
- [5] R. E. Kass, V. Ventura, and E. N. Brown. Statistical issues in the analysis of neuronal data. *Journal of Neurophysiology*, 94:8–25, 2005.
- [6] M. West. Hierarchical mixture models in neurological transmission analysis. *Journal of the American Statistical Association*, 92:587–606, 2007.
- [7] F. Rigat, M. de Gunst, and J. van Pelt. Bayesian modeling and analysis of spatio-temporal neuronal networks. *Bayesian Analysis*, pages 733–764, 2006.
- [8] D. Patnaik, P. Sastry, and K. Unnikrishnan. Inferring neuronal network connectivity from spike data: A temporal data mining approach. *Scientific Programming*, 16:49–77, 2008.
- [9] C. O. Diekman, P. S. Sastry, and K. P. Unnikrishnan. Statistical significance of sequential firing patterns in multi-neuronal spike trains. *Journal of neuroscience methods*, 182(2):279–284, 2009.
- [10] P. S. Sastry and K. P. Unnikrishnan. Conditional probability-based significance tests for sequential patterns in multineuronal spike trains. *Neural Comput.*, 22(4):1025–1059, 2010.
- [11] A. Kottas, S. Behseta, D. E. Moorman, V. Poynor, and C. R. Olson. Bayesian nonparametric analysis of neuronal intensity rates. *Journal of Neuroscience Methods*, 203(1), 2012.
- [12] R. C. Kelly and R. E. Kass. A framework for evaluating pairwise and multiway synchrony among Stimulus-Driven neurons. *Neural Computation*, pages 1–26, 2012.
- [13] R. Barbieri, M. C. Quirk, L. M. Frank, M. A. Wilson, and E. N. Brown. Construction and analysis of non-poisson stimulus-response models of neural spiking activity. *Journal of Neuroscience Methods*, 105:25–37, 2001.
- [14] R. E. Kass and V. Ventura. A spike-train probability model. *Neural Computation*, 13:1713–1720, 2001.
- [15] D. S. Reich, J. D. Victor, and B. W. Knight. The power ratio and the interval map: Spiking models and extracellular recordings. *Journal of Neuroscience*, 18(23):10090–10104, 1998.

- [16] A. L. Jacobs, G. Fridman, R. M. Douglas, N. M. Alam, P. E. Latham, G. T. Prusky, and S. Nirenberg. Ruling out and ruling in neural codes. *Proceedings of the National Academy of Sciences of the United States of America*, 106(14):5936–5941, 2009.
- [17] J. P. Cunningham, B. M. Yu, K. V. Shenoy, and M. Sahani. Inferring neural firing rates from spike trains using gaussian processes. In John C. Platt, Daphne Koller, Yoram Singer, and Sam T. Roweis, editors, *NIPS*, 2007.
- [18] P. Berkes, F. Wood, and J. Pillow. Characterizing neural dependencies with copula models. In D. Koller, D. Schuurmans, Y. Bengio, and L. Bottou, editors, *Advances in Neural Information Processing Systems 21*, pages 129–136. 2009.
- [19] A. Kottas and S. Behseta. Bayesian nonparametric modeling for comparison of single-neuron firing intensities. *Biometrics*, pages 277–286, 2010.
- [20] L. Sacerdote, M. Tamborrino, and C. Zucca. Detecting dependencies between spike trains of pairs of neurons through copulas. *Brain Res*, 1434:243–56, 2012.
- [21] C. E. Rasmussen and C. K. I. Williams. *Gaussian Processes for Machine Learning*. MIT Press, 2nd edition, 2006.
- [22] R. M. Neal. Regression and classification using Gaussian process priors. *Bayesian Statistics*, 6:471–501, 1998.
- [23] V. Ventura, C. Cai, and R. E. Kass. Statistical assessment of time-varying dependency between two neurons. *J Neurophysiol*, 94(4):2940–7, 2005.
- [24] R. E. Kass, R. C. Kelly, and W.-L. Loh. Assessment of synchrony in multiple neural spike trains using loglinear point process models. *Annals of Applied Statistics*, 5, 2011.
- [25] R. B. Nelsen. *An Introduction to Copulas (Lecture Notes in Statistics)*. Springer, 1 edition, 1998.
- [26] D. J. G. Farlie. The performance of some correlation coefficients for a general bivariate distribution. *Biometrika*, 47(3/4), 1960.
- [27] E. J. Gumbel. Bivariate exponential distributions. *Journal of the American Statistical Association*, 55:698–707, 1960.
- [28] D. Morgenstern. Einfache beispiele zweidimensionaler verteilungen. *Mitteilungsblatt für Mathematische Statistik*, 8:234–235, 1956.
- [29] Y. Ahmadian, J. W. Pillow, and L. Paninski. Efficient Markov Chain Monte Carlo methods for decoding neural spike trains. *Neural Computation*, 23(1):46–96, 2011.